Metal-induced assembly of a semiconductor-island lattice: Ge truncated pyramids on Au-patterned Si

J.T. Robinson[1,2], J.A. Liddle[2], A. Minor[3], V. Radmilovic[3], D. O. Yi[4], P. Alex Greaney[2], K. N. Long[1,2], D. C. Chrzan[1,2] and O.D. Dubon[1,2]*

[1]Department of Materials Science and Engineering, University of California, Berkeley, CA 94720

[2]Materials Sciences Division, Lawrence Berkeley National Laboratory, Berkeley, CA 94720

[3]National Center for Electron Microscopy, Lawrence Berkeley National Laboratory, Berkeley, CA 94720

[4]Applied Science and Technology, University of California, Berkeley, CA 94720.

* Corresponding Author. E-mail: oddubon@berkeley.edu

ABSTRACT

We report the two-dimensional alignment of semiconductor islands using rudimentary metal patterning to control nucleation and growth. In the Ge on Si system, a square array of sub-micron Au dots on the Si (001) surface induces the assembly of deposited Ge adatoms into an extensive island lattice. Remarkably, these highly ordered Ge islands form between the patterned Au dots and are characterized by a unique truncated pyramidal shape. A model based on patterned diffusion barriers explains the observed ordering and establishes general criteria for the broader applicability of such a directed assembly process to quantum dot ordering.

Germanium growth on silicon has been a model system to study island, or quantum dot (QD), self-assembly processes in semiconductors. Growth occurs via the Stranski-Krastanov mode due to the 4% lattice mismatch between Ge and Si and the lower surface free energy of Ge. This mode is characterized by a transition from initially layer-by-layer growth to three-dimensional island formation. Extensive investigations have been carried out on the structure and evolution of Ge islands on Si.[1-7] Generally, Ge island ensembles are observed in a random distribution and are given names based upon their shape, e.g. huts (or pyramids), domes, and super-domes.

Island growth on lithographically templated substrates has been explored in the quest for the spatial control of Ge QDs, and to varying degrees one- and two-dimensional ordering has been achieved.[8-16] The use of stencil masks to define patterns on a surface is very attractive compared to other patterning routes that typically involve multi-step, substrate-to-substrate patterning; once fabricated a stencil mask may be used many times to extend a pattern across a surface and/or generate a pattern on multiple substrates, enabling the investigation of collective phenomena in QD assemblies. The challenge then is to uncover a growth process in which the patterns generated with a stencil mask induce QD ordering. We have discovered one such process whereby Ge islands order on a Si substrate that has been patterned simply by the evaporation of Au through a stencil mask. The remarkable simplicity of the assembly process has enabled us to probe the dynamics of island ordering as well as the morphological evolution of unique island shapes.

For the experiments described here Si (001) wafers were degreased in solvents, rinsed in HF, and then mounted in an electron-beam evaporation chamber with a stencil mask placed directly in contact with the surface. One nanometer of Au was deposited through the mask, which contains arrays of square windows ranging from 75 nm to 400 nm in side length. Samples were then removed and transferred to a molecular beam epitaxy reactor for Ge deposition using an elemental Ge effusion source. The substrate was outgassed at 300°C and 600°C before Ge deposition, which typically took place at the latter temperature at a rate of ~9 ML/min. (1 ML of Ge = 6.27×10^{14} cm^{-2}).

We have investigated the growth behavior of Ge islands in two sample regions: (i) a region of Ge deposited on the Au-free Si surface and (ii) a region of Ge deposited on the Au-patterned Si surface. In the Au-free region, we find that Ge island evolution is well-described by previous reports.[3,4,7] Islanding occurs after approximately 3ML of Ge with a bimodal distribution of pyramids and domes at lower coverages (<8ML). Pyramidal islands have four {105} side facets with approximately a 1:10 (height:base) aspect ratio while domes are multi-faceted structures containing {105} and {113} side facets with a 1:5 aspect ratio. At higher coverages (>10ML), islands grow and coarsen so that only dome and super-dome islands are observed. Super-dome islands contain additional {111} facets marking the boundary to the substrate.

The presence of a gold pattern on the Si surface results in a complete change in islanding behavior. Figure 1a shows an atomic force microscopy (AFM) image of a Au-patterned Si region on which the equivalent of 11 ML of Ge was deposited. The tallest features represent Ge islands, which themselves have ordered into a square lattice. The island array extends over 10^5 μm^2, an area defined by the stencil mask. Indeed, ordered island regions are readily detected by optical diffraction as shown in Figure 1b. Each quadrant in Figure 1b contains over one-hundred thousand islands. Surprisingly the Ge islands assemble at the (½, ½)-type position of the square lattice formed by the Au pattern as revealed in Figure 1c; this is unlike the well-known vapor-liquid-solid process in which nanowire growth occurs at Au sites.[17,18] We shall refer to the position of Ge islands as center sites. Figure 1d shows the Au pattern on Si after annealing at the growth temperature (600°C) for forty-five minutes. The original pattern is clearly preserved.

The Ge islands forming the array shown in Figure 1 have an aspect ratio between 1:2 and 1:3 and a unique truncated pyramidal (TP) shape as revealed in Figure 2a. The TP shape is characterized by {111} side facets, {110} corner facets, and a (001) top facet. This island shape has been confirmed by transmission electron microscopy (TEM) as shown in Figure 2c. TP islands are relaxed via misfit dislocations and intermixing. Chemical analysis by electron dispersive spectroscopy (EDS) using a 1 nm electron beam probe revealed Si compositions up to 30 at.% in the TP islands similarly to previous

studies of Ge growth on Au-free Si (001).[19,20,21] The presence of a Ge wetting layer in the Au-patterned region has been detected as well.

Gold was not detected in the islands within the atomic-percent-level sensitivity of EDS. Nevertheless, the role of Au in producing the surprising difference in island shape cannot be discounted as even a small amount of Au on the surface may modify surface energies and drive the observed faceting. Thus far, we know that Sn can be used instead of Au to direct island organization; when Sn is used, island shapes are markedly different from the TP shape observed on Au-patterned Si. Further studies are under way.

Observations of island shape evolution at low coverages (1.5 ML-3 ML) reveal that TP islands originate from lens-like islands at center sites. The largest lens-like islands develop distinct facets marking the boundary with the substrate and evolve into TP islands that continue to grow with further deposition as well as by coarsening presumably through the consumption of the smaller islands, which disappear. Evolution of islands into the TP shape results in a dramatic change in island dimensions as shown in Figure 3. At intermediate coverages (4 ML-8 ML), one to three almost fully evolved truncated pyramidal islands are found at each center site. Above 8ML a one-TP-island-per-site relationship is widely observed (Figure 1a). We note that coherent TP islands have been observed in the growth of $Si_{1-x}Ge_x$ (for x up to 0.3) islands on Si (001) by liquid-phase epitaxy,[22,23] in which similar island growth dynamics appear to be at play. We therefore believe that the growth of SiGe islands by Ge and Si co-evaporation onto a metal-patterned substrate is likely to result in coherent (dislocation-free) island arrays.

Substrate orientation plays an important role in determining island shape. Beyond the TP shapes observed on Si (001), islands grown on Au-patterned Si (111) have an approximately tetrahedral island shape. Germanium growth on Au-patterned Si (110) results in two-fold symmetric, rod-shaped islands, which are preceded at low Ge coverages by lens-like islands. These observed shapes—TP, tetrahedral, and rod-like—are consistent with the symmetry of the growth surface.

Figure 4 shows a plot of island volume versus surface area in both the Au-patterned and Au-free regions. At an equivalent Ge coverage of 5.5 ML, the expected bimodal distribution of huts and domes is observed on Au-free Si (001). The TP islands formed in the Au-patterned region have a lower surface area (SA) to volume (V) ratio, which suggests that to first order these are energetically more stable than the hut or dome islands. At a Ge coverage of 50 ML, islands in the Au-free region have coarsened and grown to domes and super-domes while in the patterned region a shape transition of TP islands to a more super-dome-like structure has occurred as noted by the convergence of the data at larger island sizes. This transition includes the introduction of {113} as well as other facets at the top of the islands while the steeper {111} facets continue to mark the boundary with the substrate (Figure 2). These and other experiments indicate that the transition from TP to super-dome-like islands is a continuous one.

The formation of island-free regions around each Au-site is central to understanding the ordering process observed here. By varying the Au-pattern spacing we can vary the degree to which neighboring Au-site interactions occur. When the Au-pattern spacing is larger than the island-free regions, or denuded zones, island ordering is not observed (Figure 5a). Germanium islanding occurs completely around the denuded zone surrounding each Au site. When the Au spacing is decreased such that neighboring denuded zones begin to interact, the first evidence of island ordering emerges (Figure 5b); islands are confined to center sites. As the Au spacing is decreased further, a close to one-island-per-site relationship results (Figure 5c). We note that in all experiments the ratio of mass outside the denuded zones to that within is larger than one might expect if the deposited Ge is partitioned based on the areas of these two regions. This along with island ordering at center sites suggests the existence of a diffusion barrier at the denuded zone boundary.

Kinetic Monte Carlo (KMC) simulations have been performed to study the dynamics of nucleation, growth and coarsening on the patterned surface, leaving aside the issue of island morphology. A number of physical processes has been considered as the origin of the denuded zones about the Au sites and the ordering of Ge islands, including the possibility that the patterned Au sites act as strong adatom sinks and conversely as diffusion (reflecting) barriers. These scenarios fail to produce

the observed island ordering behavior. Instead, the only successful model that we have identified associates a strongly reflecting diffusion barrier with the outer boundary of the denuded zone.

The circular diffusion barriers that model the denuded zones are assumed to have the following properties. Ge adatoms directly deposited onto a barrier are incorporated into the barrier and taken out of the simulation. Ge adatoms that migrate to the barrier edge are reflected by the barrier. Ge islands overlapping with the barrier are partially incorporated into the barrier with the island size subsequently decreased. (As an island grows, its center of mass executes a random walk, and it is possible for the island to "walk" into the denuded zone.)

KMC simulations are performed on samples with proportions similar to those employed experimentally but at a smaller scale to facilitate computation. Specifically, the barrier radii are taken to be 30Å, and nearest-neighbor barrier separation distances are chosen to be 70Å, 80Å and 90Å. The coverage is set at 1/2 ML at a diffusivity to flux ratio of $D/(Fa^4)=10^5$, where D is the adatom diffusion coefficient, F is the adatom flux rate, and a is the adatom jump distance.

The interplay between denuded zones and the nucleation and growth of Ge islands is displayed in Figures 5d-f. For systems in which the radii of the denuded zones are comparable to their separation, one observes no island ordering at center sites. As diffusion barriers are brought into proximity, the islands begin to order. Ordering is pronounced once the diffusion barriers are separated by approximately 1/3 of their radii. As the barrier separation distance decreases, the nucleation allowed areas are localized to the center sites. This trend is clearly observed in both experiments and KMC simulations (Figure 5).

The physical origin and actual strength of the diffusion barriers and the formation of denuded zones are still not understood. It is very possible that dynamical changes in chemical potential across the surface as a result of factors such as island-shape transitions and strain evolution lead to conditions favorable for the formation of denuded zones and their associated diffusion barriers. These fundamental issues concerning the assembly process are the subject of continuing studies.

Both experiments and simulations indicate that ordering produces more uniform island sizes. Experimentally, the islands undergo a shape transition from lens-like to TP and finally to a super-dome-like; island shape transitions can result in a narrowing of the island-size distribution even in the case of random nucleation on bare surfaces.[4] However, the KMC simulations indicate that substrate patterning alone can narrow the size distribution as well.

The diffusion-based dynamics of this growth process means that growth temperature can be used to tune array assembly over a wide range of length scales while metal-pattern design (i.e. diffusion barrier pattering) can be exploited to form a variety of nanostructure arrays. The simplicity and diffusion-based nature of the process provides the distinct possibility of applying it to other heteroepitaxial islanding systems where an array of diffusion barriers should also lead to island ordering.

Acknowledgements. This work was supported by the LDRD Program of Lawrence Berkeley National Laboratory under the US Department of Energy Contract No. DE-AC03-76SF00098. The authors thank A. Kubota for fruitful discussions.

Figure Captions

Figure 1. (a) AFM height images showing Ge islands grown in the Au-patterned region (height scale: 100 nm; 10x10 μm^2). (b) Optical diffraction from Ge island arrays. The patterned Au spacing decreases in a clockwise fashion from the upper right red square. (c) AFM image (height scale: 100nm; 2x2 μm^2) showing the relative positions of Ge islands to the Au patterned squares. (d) Au-pattern after annealing at the growth temperature (600°C) for 45 min. (2.5x2.5 μm^2).

Figure 2. AFM phase-images of an island in the Au patterned region after (a) 5.5 ML-Ge deposition revealing a TP shape and (b) 50 ML-Ge deposition revealing a super-dome-like shape. (c) Dark-field TEM image of a Ge island taken in an $[0\bar{2}2]$ diffracting condition. Misfit dislocations can be seen along {111} planes. The pyramid itself was not sectioned. (d) AFM phase-image of a super-dome-shaped island in the Au-free region after 50 ML-Ge deposition.

Figure 3. (a) AFM phase-image in the proximity of a center site revealing the evolution of the TP island shape (labeled 1 and 2) from a lens-like island (labeled 3 and 4). (b) Horizontal cross-section (height scan) of islands shown in (a). The aspect ratio of the islands increases dramatically upon the island shape transition from lens-like to TP.

Figure 4. Island surface area versus island volume for the Au patterned (triangles) and Au-free (circles) regions after 5.5 ML (filled symbols) and 50 ML (clear symbols) of deposited Ge.

Figure 5. Effect of Au-pattern spacing on Ge island ordering observed by AFM (a, b, and c) for a deposition temperature of 500°C. In (a) the Au-spacing is greater than twice the denuded zone radius,

R_d, represented by the dotted circle, and Ge islanding occurs completely around each Au-site. In (b) the Au-spacing is slightly larger than R_d. In (c) the Au-spacing is approximately R_d and one-island-per-site ordering is almost reached. Growth and nucleation of 3-D islands determined by KMC simulations result in the corresponding island distributions shown in (d), (e), and (f). Each barrier with radius R_d (large, ordered gray circles) includes the Au site and denuded zone. Germanium island ordering emerges as the barrier separation X decreases. Scaled down lengths for these simulations are R_d = 30Å and X = 90Å, 80Å, and 70Å for (d), (e), (f), respectively. When the X = 60Å, or $2R_d$, a one-island-per-site relationship is achieved (not shown). The z-scale in the AFM images is truncated at 20nm to enhance the Ge island positions relative to the Au-sites. Similar experimental results are observed for deposition at higher substrate temperatures and wider Au pattern spacing.

References

1. Eaglesham, D. J.; Cerullo, M. *Phys. Rev. Lett.* **1990**, 64, 1943.

2. Mo, Y.-W.; Savage, D. E.; Swartzentruber, B. S.; Lagally, M. G. *Phys. Rev. Lett.* **1990**, 65, 1020.

3. Medeiros-Ribeiro, G.; Bratkovski, A. M.; Kamins, T. I.; Ohlberg, D. A. A.; Williams, R. S. *Science* **1998**, 279, 353.

4. Ross, F. M.; Tersoff, J.; Tromp, R. M. *Phys. Rev. Lett.* **1998**, 80, 984.

5. Teichert, C.; Bean, J. C.; Lagally, M. G. *Appl. Phys. A* **1998**, 67, 675.

6. Floro, J.A. *et al. Phys. Rev. Lett.* **1998**, 80, 4717.

7. Ross, F. M; Tromp, R. M.; Reuter, M. C. *Science* **1999**, 286, 1931.

8. Tersoff, J.; Teichert, C.; Lagally, M.G. *Phys. Rev. Lett.* **1996**, 76, 1675.

9. Kamins, T. I.; Williams, R. S. *Appl. Phys. Lett.* **1997**, 71, 1201.

10. Kim, E. S.; Usami, N.; Shiraki, Y. *Appl. Phys. Lett.* **1998**, 72, 1617.

11. Schmidt, O. G. *et al. Appl. Phys. Lett.* **1999**, 74, 1272.

12. Schmidt, O. G. *et al. Appl. Phys. Lett.* **2000**, 77, 4139.

13. Jin, G.; Liu, J. L.; Wang, K. L. *Appl. Phys. Lett.* **2000**, 76, 3591.

14. Kitajima, T.; Liu, B.; Leone, S. R. *Appl. Phys. Lett.* **2002**, 80, 497.

15. Yang, B.; Liu, F.; Lagally, M.G. *Phys. Rev. Lett.* **2004**, 92, 025502.

16. Zhong, Z.; Bauer, G. *Appl. Phys. Lett.* **2004**, 84, 1922.

17. Wagner, R. S.; Ellis, W. C. *Appl. Phys. Lett.* **1964**, 4, 89.

18. The difference between island and nanowire growth is at least in part due to the catalytic nature of Au in the VLS process; nanowires are most successfully grown from compound (gas) sources and not from elemental effusion sources such as the one used in the present study. In addition, island location away from Au sites is likely related to the lattice misfit between Ge and Si as we have found that Ge deposition on a Au-decorated Ge surface results in Ge island growth at Au sties.

19. Liao, X. Z. *et al. Appl. Phys. Lett.* **2000**, 77, 1304.

20. Denker, U.; Stoffel, M.; Schmidt, O.G. *Phys. Rev. Lett.* **2003**, 90, 196102.

21. Malachias, A. et al., *Phys. Rev. Lett.* **2003**, 91, 176101.

22. Hanke, M. *et al.*, *Phys. Rev. B* **2004**, 69, 075317.

23. Hanke, M. *et al.*, *Appl. Phys. Lett.* **2004**, 84, 5228.

Figure 1

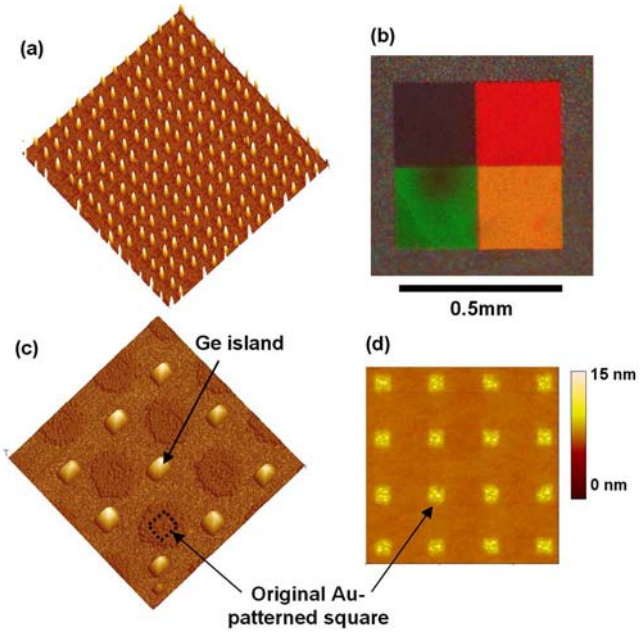

Figure 2

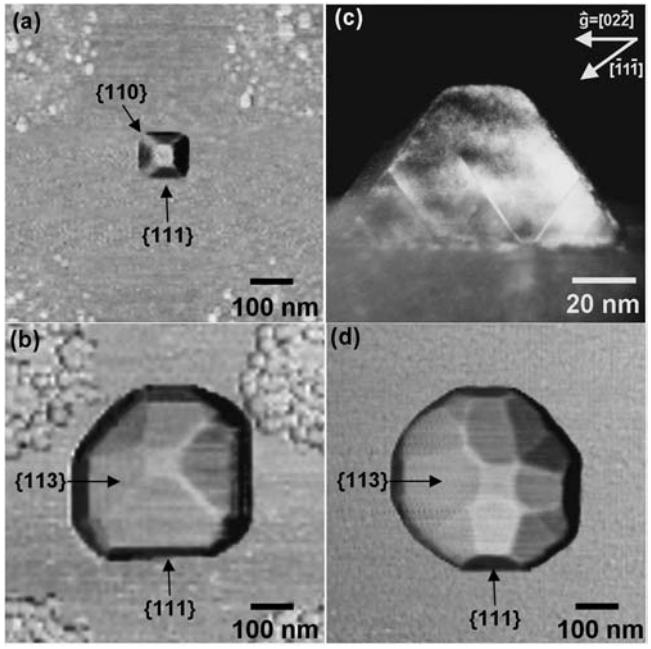
(a)
{110}
{111}
100 nm
(c)
ĝ=[02$\bar{2}$]
[1$\bar{1}$1$\bar{1}$]
20 nm
(b)
{113}
{111}
100 nm
(d)
{113}
{111}
100 nm

Figure 3

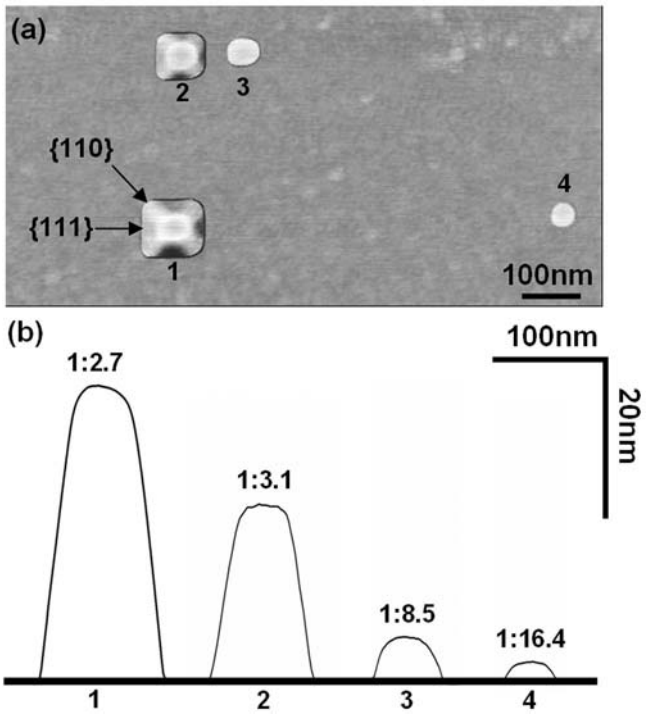

Figure 4

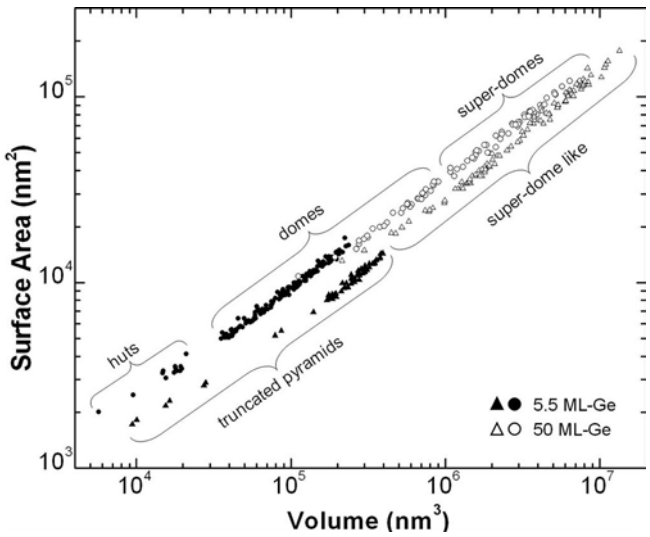
Surface Area (nm^2)
Volume (nm^3)
10^3
10^4
10^5
10^4
10^5
10^6
10^7
huts
truncated pyramids
domes
super-domes
super-dome like
5.5 ML-Ge
50 ML-Ge

Figure 5